# Proxy-Based Sliding-Mode Tracking Control of Piezoelectric-Actuated Nanopositioning Stages

Guo-Ying Gu, *Member, IEEE*, Li-Min Zhu, *Member, IEEE*, Chun-Yi Su, *Senior Member, IEEE*, Han Ding, *Senior Member, IEEE*, and Sergej Fatikow, *Member, IEEE*

***Abstract*—In this paper, a proxy-based sliding-mode control (PBSMC) approach is proposed for robust tracking control of a piezoelectric-actuated nanopositioning stage composed of piezoelectric stack actuators and compliant flexure mechanisms. The essential feature of the PBSMC approach is the introduction of a virtual coupling proxy, which is controlled by the sliding-mode controller (SMC) to track the desired position. Simultaneously, due to the virtual coupling, a proportional-integral-derivative (PID) controller on the other side of the proxy ensures the position of the end-effector of the stage to follow the position of the proxy. Therefore, the PBSMC guarantees the end-effector to track the desired trajectory. The advantages of the developed PBSMC lie in the facts that 1) the discontinuous signum function in the traditional SMC is omitted without any approximation. Hence, the output of the PBSMC is continuous, which does not suffer from the chattering phenomenon; and 2) the PBSMC laws are developed without having the necessity to include the nominal system model, hysteresis model or the state observer. Hence, the PBSMC provides a novel effective yet simple control method, which permits to avoid the lack of performances from PID and the chattering from SMC, and permits to combine the advantages from them. The stability of the closed-loop control system is proved through Lyapunov analysis. Finally, comparative studies are performed on a custom-built piezo-actuated stage. Experimental results show that the tracking errors of the PBCM are reduced by 74.22%, as compared to the traditional PID controller, with the desired sinusoidal trajectory under the 50-Hz input frequency, which clearly demonstrates the superior tracking performance of the PBSMC.**

***Index Terms*—Disturbance, hysteresis, piezo-actuated nanopositioning stage, proxy-based sliding-mode control, tracking control.**

## I. Introduction

NANOPOSITIONING, i.e., nanometer-scale precision control at dimensions of less than 100 nm, is becoming more and more significant in the fields of micro/nanotechnology applications [1], such as micro/nanomanipulators [2], [3], atomic force microscopies [4], data storage devices [5], and nanomanufacturing equipment [6]. Piezoelectric-actuated (piezo-actuated) stages composed of piezoelectric stack actuators (PSAs) and compliant flexure mechanisms are one of the enabling tools to achieve the nanopositioning owing to the fast response time and extremely fine positioning resolution of PSAs. However, the inherent hysteresis nonlinearity of the PSAs and vibration dynamics of the stages lead to the control challenge of the piezo-actuated stages [1], [7].

It has been experimentally verified that driving the PSAs with the charge amplifier can greatly eliminate the hysteresis nonlinearity [8], [9]. However, the utilization of the charge amplifier introduces the implementation complexity and cost. Hence, the VA is still most widely employed to drive the PSAs. In the VA driven case, the hysteresis nonlinearity can induce a positioning error which is more than 15% of the stage's displacement range. During the past decade, various control approaches have been proposed to enable the nanopositioning motion of the piezo-actuated stages.

Feedforward control with the inverse hysteresis models is the most commonly used approach to mitigate the hysteresis effect [10]. In the literature, many hysteresis models such as Preisach models [1], [11], Prandtl-Ishlinskii models [12], [13], Duhem models [14] and Bouc–Wen models [15], are developed to describe the hysteresis effect, which are then used to construct the inverse models for hysteresis compensation. In practice, feedback control such as PID control [2], [16], PD/lead-lag control [17], repetitive control [18], servocompensator/stabilizing control [19] is usually applied in combination with the feedforward control to handle the inverse compensation errors and the remaining dynamics of the piezo-actuated stages. However, it is generally complicated to identify an accurate hysteresis model and even difficult to construct its inverse. This motives the researchers to develop robust feedback control approaches, such as LQG control [20], $H_\infty$ control [21], disturbance observer control [22], sliding-mode control (SMC) [23]–[26], and robust adaptive control [27], where the hysteresis nonlinearity is treated as a disturbance to the nominal model of the linear dynamics systems. In these robust control approaches, SMC is more attractive owing to the ease of implementation and robustness against unknown disturbances. However, the main problem of the SMC is the existence of the discontinuous signum function, which may lead to chattering in practice. To alleviate the chattering phenomenon, boundary layer control approaches are generally adopted to replace the signum function with the continuous saturation functions [23]–[26]. It is noted that the sliding function of the SMC is usually defined by a proportional and derivative

Manuscript received January 27, 2014; revised September 15, 2014; accepted September 23, 2014. Date of publication October 15, 2014; date of current version August 12, 2015. Recommended by Technical Editor S. O. R. Moheimani. This work was supported in part by the National Natural Science Foundation of China under Grant 51405293, Grant 91023047, and Grant U1201244.

G.-Y. Gu, L.-M. Zhu, and H. Ding are with the State Key Laboratory of Mechanical System and Vibration, School of Mechanical Engineering, Shanghai Jiao Tong University, Shanghai 200240, China (e-mail: guguoying@sjtu.edu.cn; zhulm@sjtu.edu.cn; hding@sjtu.edu.cn).

C.-Y. Su is with the Department of Mechanical and Industrial Engineering, Concordia University, Montreal, QC H3G1M8, Canada (e-mail: cysu@alcor.concordia.ca).

S. Fatikow is with the Division of Microrobotics and Control Engineering, University of Oldenburg, Oldenburg 26129, Germany (e-mail: fatikow@uni-oldenburg.de).

Color versions of one or more of the figures in this paper are available online at http://ieeexplore.ieee.org.

Digital Object Identifier 10.1109/TMECH.2014.2360416

control action based on the output or output error. To achieve the better tracking accuracies of the piezo-actuated stages, recent works tried to design new sliding functions with the integral control action [25], [26], [28]. However, due to the fact that only the position information of the piezo-actuated stages is available in practice, it is generally necessary to design an additional state observer [26] or model predictive controller [25], [28], which further increases the complexity of the developed controllers.

In this paper, a novel proxy-based sliding mode control (PBSMC) approach introduced by Kikuuwe and Fujimoto [29] is proposed for high-precision tracking control of piezo-actuated stages. The essential feature of the proposed PBSMC approach is that it can be viewed as an alternative approximation of the conventional SMC as well as an extension of PID control by introduction of a virtual objective (proxy) so that the resulting control laws have the advantages of each approach but not their disadvantages: only the output position is used as feedback, and zero steady-state tracking error is ensured. The stability of the developed PBSMC approach is proved through Lyapunov analysis, and experimental results on a custom-built piezo-actuated stage show that the PBSMC achieves the superior tracking performance. To the best knowledge of the authors, this paper is the first attempt at introducing the PBSMC approach for nanopositioning control of piezo-actuated stages composed of PSAs and compliant flexure mechanisms.

Unlike the existing SMC [23], [24] and integral type SMC approaches [25], [26], [28] for piezo-actuated stages, the distinct advantages of the PBSMC approach are as follows.

1) Only the output position of the piezo-actuated stage is sufficient for implementation, whereas the nominal system model, hysteresis model or the state observe does not appear in the PBSMC algorithms. Therefore, the PBSMC has a very good disturbance rejection capability, which can be implemented as simply as the PID control but with the improved tracking performance than the PID control.
2) To avoid the chattering phenomenon of the SMC, boundary layer methods [23]–[26] are generally applied. With the relation expressed in (21), the discontinuous signum function in the traditional SMC is directly omitted without any approximation. Hence, the output of the PBSMC is continuous, which does not suffer from the chattering phenomenon.
3) The traditional SMC for piezo-actuated stages may cause the nonzero steady-state error problem [25], [26], [28]. To overcome this problem, novel sliding functions with the integral control action are designed in new SMC development [25], [26], [28]. Experimental results as shown in Figs. 7 and 10 obviously demonstrate that the PBSMC does not suffer this problem. Therefore, it is not necessary to develop the new SMC with novel integral-type sliding functions.

In the rest of this paper, the problem formulation is presented in Section II. The design procedure and stability analysis of the PBSMC is outlined in Section III. Section IV describes the experimental setup and verifies the development with the experimental studies. Finally, conclusions are provided in Section V.

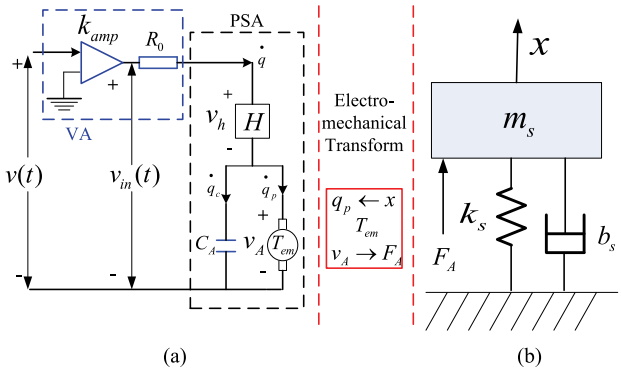


Fig. 1. General dynamic model of a piezo-actuated stage [27]. (a) Electrical aspect (b) Mechanical aspect.

## II. Problem Formulation

### A. Dynamic Modeling

A general dynamic model of the piezo-actuated stage, including frequency response of the stage, voltage-charge hysteresis and nonlinear electric behavior, has been recently developed in [27]. Considering the piezo-actuated stage driven by the voltage amplifier (VA), this general model, as shown in Fig. 1, can be described by the following set of equations [27]:

$$R_0\dot{q}(t) + v_h(t) + v_A(t) = k_{\rm amp}v(t) \tag{1}$$

$$v_h(t) = H(q) \tag{2}$$

$$q(t) = q_c(t) + q_p(t) \tag{3}$$

$$v_A(t) = q_c(t)/C_A \tag{4}$$

$$q_p(t) = T_{\rm em}x(t) \tag{5}$$

$$F_A = T_{\rm em}v_A(t) \tag{6}$$

$$m_s\ddot{x}(t) + b_s\dot{x}(t) + k_s x(t) = F_A \tag{7}$$

where $v(t)$ is the voltage of the control input; $k_{\rm amp}$ and $R_0$ are the fixed gain and equivalent internal resistance of the VA, respectively; $T_{\rm em}$ represents the piezoelectric effect, which is an electromechanical transducer with transformer ratio; $v_A$ is the voltage related to the transducer; $v_h$ is the generated voltage due to the hysteresis effect $H$; $C_A$ represents the sum of the capacitances of the PSA, which is electrically parallel with the transformer; $q$ is the total charge in the PSA and the resulting current flowing through the circuit is $\dot{q}$; $q_c$ is the charge stored in the linear capacitance $C_A$; $q_p$ is the transduced charge from the mechanical side due to the piezoelectric effect; $F_A$ is the transduced force on the moving part of the stage from the electrical side; $m_s$ is the equivalent mass of the moving part of the stage, $b_s$ and $k_s$ are the equivalent damping coefficient and stiffness of the mechanism of the stage; and $x(t)$ is the output displacement of the end-effector of the stage.

From (1)–(7), the following equations can be obtained:

$$m_s\ddot{x}(t) \ + b_s\dot{x}(t) + (k_s + \frac{T_{\rm em}^2}{C_A})x(t) = \frac{T_{\rm em}}{C_A}q(t) \tag{8}$$

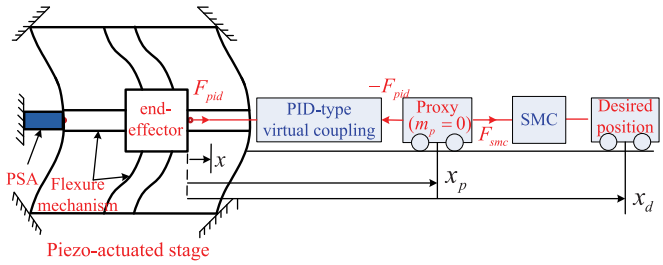


Fig. 2. Principle of the PBSMC for a piezo-actuated stage.

$$R_0 C_A \dot{q}(t) \ + q(t) - T_{\rm em} x(t) = C_A [k_{\rm amp} v(t) - v_h(t)]. \tag{9}$$

In practice, the equivalent internal resistance $R_0$ is usually assumed as $R_0 = 0$ [23], [25], [26], [28], [30]. Therefore, the electromechanical dynamic model (8) and (9) can be reduced to

$$m_s \ddot{x}(t) + b_s \dot{x}(t) + k_s x(t) = f(t) + d(t). \tag{10}$$

where $f(t) = T_{\rm em} k_{\rm amp} v(t)$ and $d(t)$ denotes the bounded disturbances including the nonlinear hysteresis effect $v_h(t)$ and external perturbation.

*Remark:* It should be noted that the PSAs also suffer from the creep nonlinearity, which is a slower drift phenomenon of the output displacement of PSAs over extended periods when subjected to a constant applied voltage [1]. It is pointed out that this phenomenon can be easily mitigated by a traditional feedback controller, such as a conventional PID controller [16], [31], Thereafter, the creep nonlinearity is generally neglected in the dynamic models of the piezo-actuated stages [21], [23]–[27].

### B. Control Objective

The dynamic model (10) shows that the piezo-actuated stage is described by a linear second-order model, where the hysteresis effect is involved in the unknown disturbances $d(t)$. Consider the system (10), the tracking objective in this paper is stated as follows: In the presence of unknown disturbances involving with the hysteresis nonlinearity, design a control law $f(t)$ so that the stage's output $x(t)$ follows the desired trajectory $x_d(t) \in \mathcal{C}^2$, i.e., $x(t) \to x_d(t)$ as $t \to \infty$. To achieve this control objective, a PBSMC law will be designed in the following development. It is pointed out that, for brevity, the time variable $t$ is generally omitted in the following development.

## III. PBSMC Design

In this section, the design procedure and stability analysis of the PBSMC for the PSA-actuated stage are presented.

### A. Principle of PBSMC

The PBSMC was first developed by Kikuuwe and Fujimoto [29], [32] for robotics, which can achieve the responsive and accurate tracking capability during normal operation with smooth, slow, and safe recovery from large position errors. The principle of the PBSMC is schematically illustrated in Fig. 2. The actual controlled object is connected to a virtual object, which is referred to as a proxy, by means of a PID-type virtual coupling (a PID controller). The PID controller, thus, causes an interaction force $F_{\rm pid}$ between the end effector and proxy. At the same time, the proxy is also controlled by a sliding-mode controller, which exerts the force $F_{\rm smc}$, to track the desired trajectory.

As shown in Fig. 2, $x_p$ and $\dot{x}_p$ are proxy's position and velocity, and $x_d$ and $\dot{x}_d$ are the desired position and velocity, respectively. The SMC law that is used to control the virtual proxy is given by

$$F_{\rm smc} = F {\rm sgn}(\sigma_1) \tag{11}$$

with the sliding surface $\sigma_1$ defined as

$$\sigma_1 = x_d - x_p + \lambda(\dot{x}_d - \dot{x}_p) \tag{12}$$

where sgn is the signum function, $F > 0$ and $\lambda > 0$ are designed control gains. It is straightforward (see, for example, Chapter 7 of the Slotine and Li's book [33] for an introduction to SMC) that once the proxy has reached the sliding surface $\sigma_1 = 0$, the error dynamics is determined by

$$x_d - x_p + \lambda(\dot{x}_d - \dot{x}_p) = 0. \tag{13}$$

Therefore, the position error $(x_d - x_p)$ and velocity error $(\dot{x}_d - \dot{x}_p)$ of the proxy will exponentially converge to zero with the time constant $\lambda > 0$, which indicates that the proxy gently converges to its desired trajectory.

On the other hand, the force produced by the PID controller is

$$F_{\rm pid} = k_p(x_p - x) + k_i \int_0^t (x_p - x) d\tau + k_d(\dot{x}_p - \dot{x}) \tag{14}$$

where $x$ and $\dot{x}$ are the end effectors actual position and velocity, $k_p$, $k_i$ and $k_d$ are designed positive gains of the PID controller.

By defining

$$a = \int_0^t (x_p - x) d\tau \tag{15}$$

and

$$\sigma = x_d - x + \lambda(\dot{x}_d - \dot{x}) \tag{16}$$

(11) and (14) can be, respectively, rewritten as

$$F_{\rm smc} = F {\rm sgn}(\sigma - \dot{a} - \lambda \ddot{a}) \tag{17}$$

and

$$F_{\rm pid} = k_p \dot{a} + k_i a + k_d \ddot{a}. \tag{18}$$

It should be noted that the fact $\sigma_1 = \sigma - \dot{a} - \lambda \ddot{a}$ is used in the above equations.

Considering the proxy, the equation of motion can be governed by

$$m_p \ddot{x}_p = F_{\rm smc} - F_{\rm pid}. \tag{19}$$

According to (11)–(19), the block diagram of the PBSMC is shown in Fig. 3. It should be pointed out that if one directly implements the controllers using (17) and (18), the motion of the virtual proxy mass would have to be simulated in software. In practice, Kikuuwe and Fujimoto [29], [32] realized them by

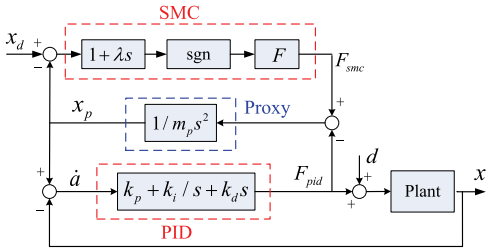


Fig. 3. Control block of the PBSMC.

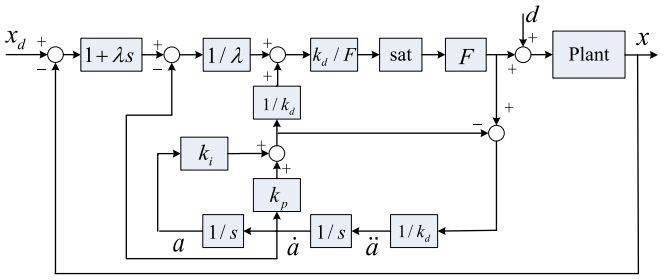


Fig. 4. Equivalent control block of the PBSMC depicted for real-time implementation.

setting the proxy mass in (19) to be zero. Then, $F_{\rm smc} = F_{\rm pid} \equiv f$ is satisfied. Thereafter, the PBSMC law is obtained by

$$f = k_p\dot{a} + k_i a + k_d\ddot{a} = F\mathrm{sgn}(\sigma - \dot{a} - \lambda\ddot{a}). \tag{20}$$

In the upcoming derivations, the following relation of signum function sgn and the saturation function sat will be used [32]:

$$\begin{aligned} y + Xw = \; & Y\mathrm{sgn}(z - Zy) \\ \Leftrightarrow \quad y = \; & -Xw + Y\mathrm{sat}(\frac{z/Z + Xw}{Y}) \end{aligned} \tag{21}$$

with

$$\mathrm{sat}(y) = \begin{cases} \mathrm{sgn}\,(y), & \text{if } |y| > 1 \\ y, & \text{if } |y| \le 1 \end{cases} \tag{22}$$

where $X, Y, Z > 0$ and $w, y, z \in \mathbb{R}$.

In the view of (21), $\ddot{a}$ in (20) can be taken out as follows:

$$\ddot{a} = -\frac{k_p\dot{a} + k_i a}{k_d} + \frac{F}{k_d}\mathrm{sat}\left(\frac{k_d}{F}\left(\frac{\sigma - \dot{a}}{\lambda} + \frac{k_p\dot{a} + k_i a}{k_d}\right)\right). \tag{23}$$

Therefore, the control law (20) can be rewritten as

$$f = F\mathrm{sat}\left(\frac{k_d}{F}\left(\frac{\sigma - \dot{a}}{\lambda} + \frac{k_p\dot{a} + k_i a}{k_d}\right)\right). \tag{24}$$

In order to real-time implement the control laws (15), (16), (23), and (24), Fig. 4 depicts the equivalent control block of the PBSMC scheme shown in Fig. 3.

In view of (11)–(24), the control algorithm of PSMC is the analytical solution for the differential algebraic constraints that result from the imaginary dynamical system by introducing the virtual object, called proxy [29], [32]. The essential feature of the PBSMC is that it can be viewed as an alternative approximation of the conventional SMC and also an extension of PID control. The main benefits are that small position errors can be remedied by the well-tuned PID controller (determined by control gains $k_p$, $k_i$, and $k_d$), and large positioning errors can be rapidly recovered owing to the SMC with the control gain $\lambda$. As a result, responsive and accurate tracking can be achieved by the PBSMC.

*Remarks:*

1) It should be noted that the main problem of the SMC is the existence of the discontinuous signum function, which may lead to chattering in practice. To avoid the chattering phenomenon, many efforts have to be made to replace the signum function. However, in the PBSMC laws, (20) and (24) are algebraically equivalent, which implies that the discontinuous function in (20), in fact, does not produce discontinuity. This is the essential difference of PSMC (20) and (24) from the conventional sliding-mode controller, which includes discontinuity that cannot be removed without approximation. Hence, the output of the PBSMC is continuous, which does not suffer from the chattering phenomenon.
2) It should be noted that an important feature of PSMC (20), or equivalently (24), is that it is an alternative approximation of a conventional SMC. For instance, by setting $k_p \to \infty$, the PMSMC law (20) degenerates to the conventional SMC with the form of $f = F\mathrm{sgn}(x_d - x + \lambda(\dot{x}_d - \dot{x}))$ [29], [32]. In addition, the PBSMC is also an extension of PID control. For instance, by setting $\lambda = \frac{k_d}{k_p}$ and $k_i = 0$, the PMSMC law (24) is equivalent to the traditional PID controller with force limitation [32], [34]. Since this paper focuses on the PBSMC approach for nanopositioning control of piezo-actuated stages, the detailed behavior descriptions and equivalent control examples of the PBSMC can be founded in, for example, [29], [32], [34], [35].
3) It should be noted that the pure differentiator as shown in Fig. 4 is generally not practical applicable due to its nonproper nature, which does not restrict high-frequency gains. Hence, it will result in a theoretically infinite high control signal when a step change of the reference or disturbance occurs [36]. To overcome this drawback, the differentiator should be filtered in practice, e.g., by $s/(1+\tau s)$ with $\tau > 0$, as in [36] for more detailed discussions and selections. It is worthy of mentioning that the dSPACE-DS1103 control system is utilized in this paper to implement the designed controller. Therefore, the filtering on the differentiator is not considered in this paper and automatically performed by the dSPACE-DS1103 control system.

### B. Stability Analysis of PBSMC

Define the tracking error and the error vectors as

$$\begin{aligned} e = \; & x_d - x \\ E = \; & [e \quad E_1] \end{aligned} \tag{25}$$

where $E_1 = [\dot{e} \;\; \ddot{a} \;\; \dot{a}]$.

Then, an error dynamics equation is obtained by using (25) and (10)

$$m_s\ddot{e} + b_s\dot{e} + k_s e = -f + \phi \tag{26}$$

with

$$\phi = m_s\ddot{x}_d + b_s\dot{x}_d + k_s x_d - d \tag{27}$$

where $|\phi| \leq \delta_0$ is satisfied with $\delta_0 > 0$.

In order to demonstrate the stability of the developed PBSMC laws for piezo-actuated stages, the following *Lemma* is introduced.

*Lemma [32]:* Considering the closed-loop system composed of the plant (26) and a PID controller (20) that accepts an input $u = \dot{x}_p - \dot{x}_d$, there exists $k_p > 0, k_i > 0$ and $k_d > 0$ that allows that the function $V_p$ satisfies

$$V_p(E_1) \geq \delta \parallel E_1 \parallel^2 \tag{28}$$

$$\dot{V}_p(E_1) \leq fu - \rho_E \parallel E_1 \parallel^2 - \rho_u \parallel u \parallel^2 \tag{29}$$

where $\rho_E$ and $\rho_u$ are positive function.

*Remark:* The *Lemma* is directly adopted from the *Conjecture* in [32]. This is because the linear portion of the system in this paper is only a special case in [32], where $C(p, \dot{p})$ in [32] becomes zero and then this conjecture can be proved and is not a conjecture anymore. For the details, please refer to [32].

*Theorem 1:* For a piezo-actuated stage described by (10) in the presence of the unknown disturbance involving with the hysteresis, with the introduction of the *Lemma*, the tracking error $e$ defined in (25) satisfies $e \to 0$ as $t \to \infty$ by applying the developed PBSMC laws (15), (16), (20), (23), and (24) as shown in Fig. 4.

*Proof:* See Appendix.

## IV. Experimental Verification

In this section, the effectiveness of the developed PBSMC laws will be verified by comparative experimental studies on a piezo-actuated nanopositioning stage.

### A. Experimental Setup

In this paper, a custom-built piezo-actuated stage composed of the PSAs and a *XY* parallel-kinematic mechanism is adopted to conduct experiments for validation of the developed PBSMC laws.

The stage is designed with two kinematic chains and each kinematic chain is composed of two symmetrically distributed flexure modules [37], which is schematically shown in Fig. 5. In each flexure module, a fixed–fixed beam and a parallelogram flexure are adopted as two orthogonal prismatic joints. Instead of using the constant rectangular cross-sectional beam, a novel center-thickened beam with larger stiffness is designed as the fixed–fixed beam to achieve high resonance frequencies of the mechanism. The center-thickened beam is also utilized to reduce the cross-coupling between two axes. In addition, a symmetric

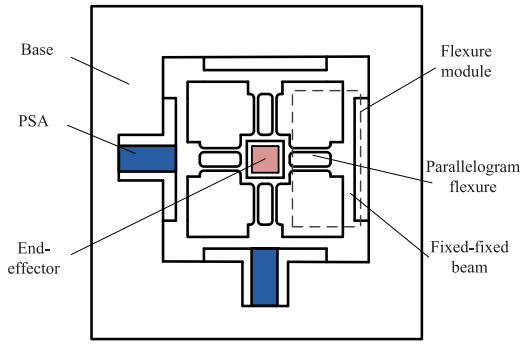


Fig. 5. Mechanical structure of the piezo-actuated stage.

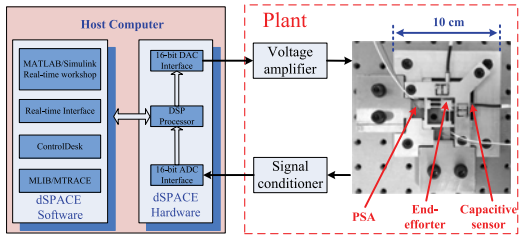


Fig. 6. Experimental setup.

configuration is adopted for the parallelogram flexures to decouple the motion in two axes totally. Experimental tests demonstrate that the workspace of the stage is 11.2 $\mu$m $\times$ 11.6 $\mu$m with the maximum cross-coupling between *X*- and *Y*-axis lower than 0.52%. Therefore, the designed stage is well decoupled; thus, the two-axis motions can be treated independently. For the purpose of verifying the proposed control laws, only the treatment of *x*-axis tracking control is presented in this paper.

In this paper, a dSPACE-DS1103 control board equipped with the 16-bit analog-to-digital converters (ADCs) and 16-bit digital-to-analog converters (DACs) is used to implement the developed control laws. The DACs produce the analog control input and the high-VA with a fixed gain of 20 is adopted to provide excitation voltage 0–200 V for driving the PSAs. Capacitive sensors (Probe 2823 and Gauging Module 8810 from MicroSense, range of +/−10 $\mu$m with analog output of +/−10 V) are utilized to real-time measure the position of the end-effector of the stage with the sensitivity of 1 V/$\mu$m. The sensor output signals are then captured by a signal conditioner and simultaneously acquired by the ADCs for the feedback control laws. Furthermore, the MATLAB/Simulink software is used to implement the control laws, which are directly downloaded to the DS1103 control board via the ControlDesk interface for real-time applications. The sampling frequency of the feedback loop is set as 20 kHz. Fig. 6 shows the block diagram of the experimental setup.

### B. Experimental Studies

The tracking performance of the developed controller is evaluated by comparative experiments in this section.

As discussed in Section III, the PBSMC is developed as the combination of the PID and SMC, and the performance of the PBSMC depends on the control gains of the PID controller. In the literature, many tuning methods such as the trial-and-error method [36], the Ziegler and Nichols tuning method [38], the $H_\infty$ constraint optimization method [39], and the optimum gain and phase margin tuning method [40], have been developed to obtain the optimum gains of the PID controller. Without losing generality, the control gains $k_p = 0.1$, $k_i = 6000$, and $k_d = 0.000001$ are tuned by the trial-and-error method in this paper to obtain a satisfied tracking performance of the piezo-actuated stage with the 1-Hz desired trajectory. It should be noted that although the selected gains of the PID controller may not be the most optimum, the same values of these gains are also adopted for the PBSMC. Then, we can fairly compare tracking performances with PID control and PBSMC under the same desired trajectories.

Fig. 7 shows tracking results with PID control (indicated by the red dash line) using the 1-Hz desired trajectory. It can be obtained from Fig. 7 that the maximum error (ME) and root-mean-square error (RMSE) with PID control is 4.9 and 1 nm, which are 0.25% and 0.05% of the displacement range, respectively.

In the PBSMC, the tuned gains $k_p$, $k_i$, and $k_d$ of the PID controller are directly used and the rest control parameters of the PBSMC are selected as $F = 1$ and $\lambda = 0.0002$ through experimental studies. As a comparison, Fig. 7 also shows the tracking results with the PBSMC indicated by the black dot line. It can be gotten that the ME and RMSE are 4.8 and 0.71 nm, respectively, which are 0.24% and 0.035% of the displacement range. It can be seen that both the PID control and PBSMC are effective to follow the 1-Hz sinusoidal trajectory. Further, control signals with PID control and PBSMC are compared in Fig. 8. It can be intuitively seen that they produce nearly identical results. This also explains why the tracking errors with the PID control and PBSMC are almost equal. For quantitatively comparing differences of them, the following definition DF is introduced with the control signal of the PID controller as the reference

$$\mathrm{DF} = \frac{\max(v_{\mathrm{pid}} - v_{\mathrm{pbsmc}}) - \min(v_{\mathrm{pid}} - v_{\mathrm{pbsmc}})}{\max(v_{\mathrm{pid}}) - \min(v_{\mathrm{pid}})} = 0.65\% \tag{30}$$

where $v_{\mathrm{pid}}$ and $v_{\mathrm{pbsmc}}$ represent the control signals with the PID control and PBSMC, respectively.

It should be mentioned that when the input frequencies of the desired trajectory is low enough, the effectiveness of the PID control for piezo-actuated stage has also been verified in the reported works such as [18], [19], [25], [26], [28]. In this paper, this test is used to demonstrate that the control gains of the PID controller are well tuned. However, the hysteresis nonlinearly caused errors ($h/H$) as shown in Fig. 9 become serious with the increase of the input frequencies. In this case, the PID control generally loses its effectiveness. It is also the motivation of this paper to develop a new control approach. In the following,

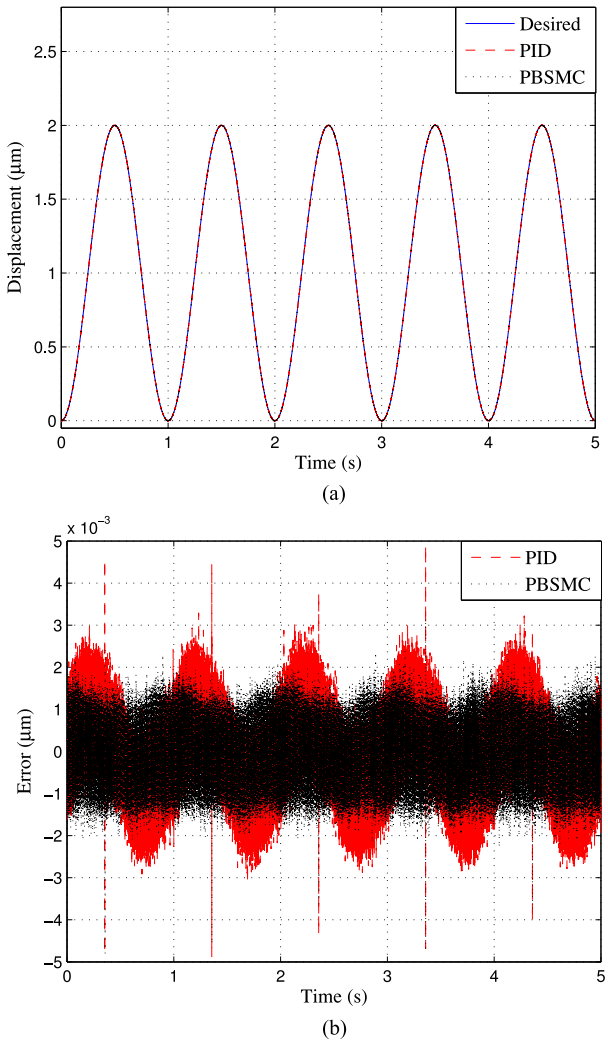


Fig. 7. Tracking results of the PID control and PBSMC with the 1-Hz sinusoidal desired trajectory. (a) Trajectory tracking. (b) Tracking error.

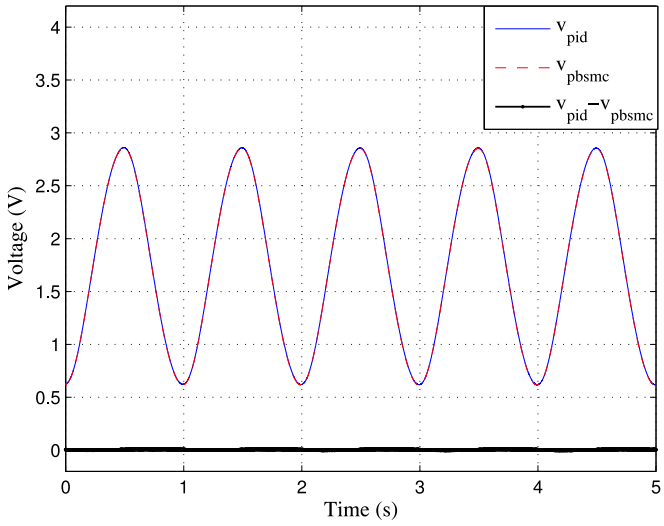


Fig. 8. Comparisons of control signals of PID controller and PBSMC with the 1-Hz sinusoidal desired trajectory.

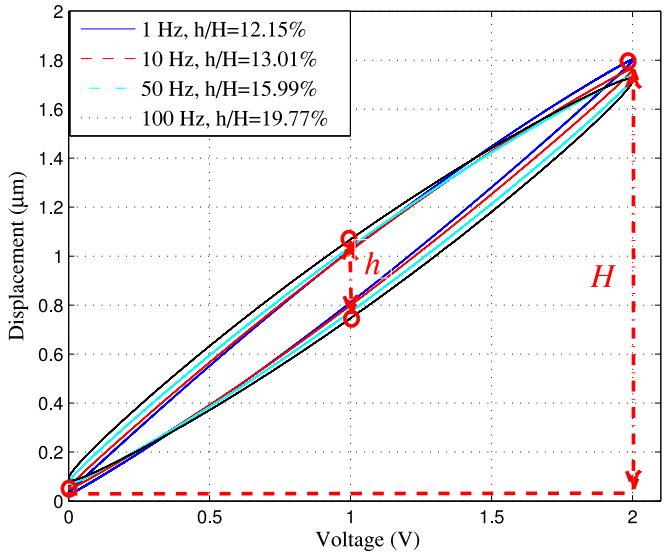


Fig. 9. Open-loop hysteresis with sinusoidal input reference under different frequencies.

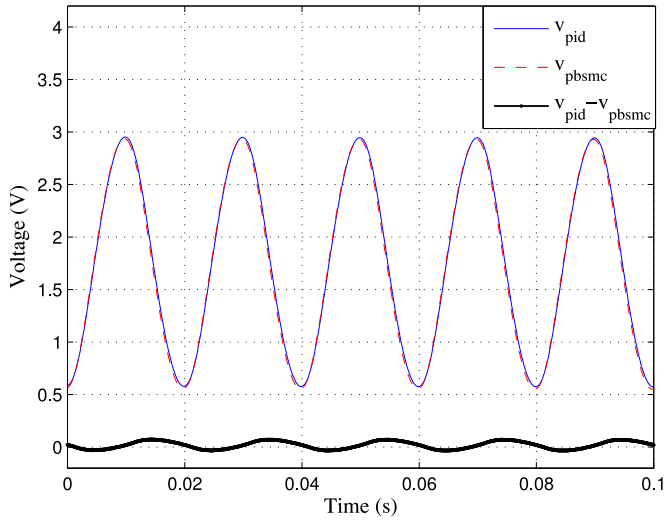


Fig. 11. Comparisons of control signals of PID controller and PBSMC with the 50-Hz sinusoidal desired trajectory.

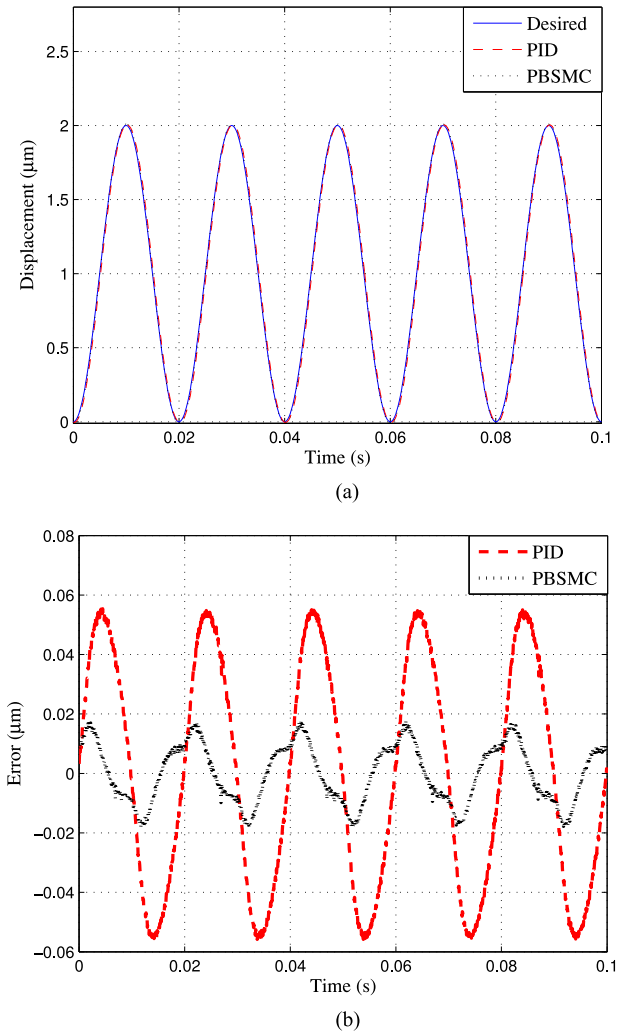


Fig. 10. Tracking results of the PID control and PBSMC with the 50-Hz sinusoidal desired trajectory. (a) Trajectory tracking. (b) Tracking error.

TABLE I
RMSEs OF THE PID CONTROL AND PBSMC UNDER DIFFERENT INPUT FREQUENCIES

| Frequencies | 1 Hz | 10 Hz | 50 Hz | 100 Hz |
|---|---|---|---|---|
| PID | 1 nm | 7.4 nm | 38.4 nm | 78.5 nm |
| PBSMC | 0.71 nm | 1.4 nm | 9.9 nm | 28.7 nm |

experimental tests under increasing input frequencies will be conducted with the same designed control gains. The results of both PID control and PBSMC will also be shown to evaluate their tracking errors and robustness.

As an illustration, Fig. 10 shows the tracking results of the PID control and PBSMC with the 50-Hz sinusoidal desired trajectory. The RMSEs of the PID control and PBSMC are 38.4 and 9.9 nm respectively, which are 1.92% and 0.5% of the displacement range. It is obvious that, comparing with the PID control, the developed PBSMC reduces the RMSE by 74.22% under the input frequency of 50 Hz, i.e., the tracking accuracy of the PBSMC is almost four times better than the PID control. In addition, Fig. 11 shows the control signals with PID control and PBSMC, respectively. From the definition in (30), we can see that the difference of the control signals is $DF = 4.39\%$. It is almost seven times larger than the one with the 1-Hz sinusoidal desired trajectory. We can also show that the larger difference of the control signals result in larger differences of the tracking errors with the PID control and PBSMC. Furthermore, Table I lists the comparison of RMSEs under different input frequencies. It can be seen from Table I that the RMSEs with PID control are 1.4, 5.2, 3.9, and 2.7 times larger than the RMSEs with PBSMC under 1, 10, 50, and 100 Hz input frequencies, respectively. Therefore, it can be obviously demonstrated that the PBSMC greatly

improves the tracking performance with the increasing input frequencies.

## V. Conclusion

This paper proposes a novel PBSMC approach for precision tracking control of a piezo-actuated nanopositioning stage without modeling the hysteresis nonlinearity. The essential feature of the PBSMC is that it can be viewed as an alternative approximation of the conventional SMC and also an extension of PID control. In this sense, the discontinuous signum function in the conventional SMC is omitted without any approximation, which results in the continuous control signal. Hence, the chattering phenomenon is avoided. As a result, smooth, fast, and accurate tracking can be achieved by the developed PBSMC laws. In addition, the PBSMC laws without using the state observer can be simply implemented in real time since the nominal system model or hysteresis model does not appear. The stability of the developed PBSMC laws is proved through Lyapunov analysis, and the effectiveness is verified by real-time comparative experiments on a custom-built piezo-actuated stage.

## Appendix
## Proof of Theorem 1

*Proof:* To demonstrate the stability of the developed control laws, a Lyapunov function candidate is defined as

$$V(E) = V_p(E_1) + \parallel F(e - \dot{a}) \parallel_1 \tag{31}$$

where $E$ and $E_1$ are defined in (25), $V_p(E_1) \geq \delta \parallel E_1 \parallel^2$ is defined in (28). Thus, it is obvious that $V(E) = 0$ when $E = \mathbf{0}$, and $V(E) > 0$ for any $E \neq \mathbf{0}$.

The time derivative of (31) can be expressed as

$$\dot{V}(E) = \dot{V}_p(E_1) + (\dot{e} - \ddot{a})F\mathrm{sgn}(e - \dot{a}). \tag{32}$$

According to the conclusion in (29), (32) can derive to

$$\begin{aligned}\dot{V}(E) \leq\ & fu - \rho_E \parallel E_1 \parallel^2 - \rho_u \parallel u \parallel^2 \\ & + (\dot{e} - \ddot{a})F\mathrm{sgn}(e - \dot{a}).\end{aligned} \tag{33}$$

By instituting (20) into (33) and using the fact $u = \dot{x}_p - \dot{x}_d = \ddot{a} - \dot{e}$, one can obtain

$$\begin{aligned}\dot{V}(E) \leq\ & (\ddot{a} - \dot{e})F\mathrm{sgn}(\sigma - \dot{a} - \lambda\ddot{a}) - \rho_E \parallel E_1 \parallel^2 - \rho_u \parallel u \parallel^2 \\ & + (\dot{e} - \ddot{a})F\mathrm{sgn}(e - \dot{a}).\end{aligned} \tag{34}$$

Considering $\sigma - \dot{a} - \lambda\ddot{a} = e - \dot{a} + \lambda(\dot{e} - \ddot{a})$, (34) becomes

$$\begin{aligned}\dot{V}(E) \leq\ & \lambda(\dot{e} - \ddot{a})\frac{F}{\lambda}[\mathrm{sgn}(e - \dot{a}) - \mathrm{sgn}(e - \dot{a} + \lambda(\dot{e} - \ddot{a}))] \\ & - \rho_E \parallel E_1 \parallel^2 - \rho_u \parallel u \parallel^2 \\ \leq\ & - \rho_E \parallel E_1 \parallel^2 - \rho_u \parallel u \parallel^2 \leq 0.\end{aligned} \tag{35}$$

It should be noted that the following relation has been used to obtain the above equation

$$y^T X[\mathrm{sgn}(z + y) - \mathrm{sgn}(z)] \geq 0 \tag{36}$$

where $X > 0$ and $y, z \in \mathbb{R}$.

Therefore, the stability of the closed-loop control system is proved, and the tracking error $e$ converges to zero as $t \to \infty$.

## References


[1] G. Y. Gu, L. M. Zhu, C. Y. Su, H. Ding, and S. Fatikow, "Modeling and control of piezo-actuated nanopositioning stages: A survey," *IEEE Trans. Autom. Sci. Eng.*, DOI: 10.1109/TASE.2014.2352364, pp. 1–20, 2014, in press.

[2] H. Tang and Y. Li, "A new flexure-based y $\theta$ nanomanipulator with nanometer-scale resolution and millimeter-scale sorkspace," *IEEE/ASME Trans. Mechatron.*, DOI: 10.1109/TMECH.2014.2342752, pp. 1–11, 2014, in press.

[3] Y. Tian, B. Shirinzadeh, D. Zhang, and G. Alici, "Development and dynamic modelling of a flexure-based Scott-Russell mechanism for nanomanipulation," *Mech. Syst. Signal Process.*, vol. 23, no. 3, pp. 957–978, 2009.

[4] Y. K. Yong, S. O. R. Moheimani, B. J. Kenton, and K. K. Leang, "Invited review article: High-speed flexure-guided nanopositioning: Mechanical design and control issues," *Rev. Sci. Instrum.*, vol. 83, no. 12, p. 121101, 2012.

[5] E. Eleftheriou, "Nanopositioning for storage applications," *Annu. Rev. Control*, vol. 36, no. 2, pp. 244–254, 2012.

[6] B. A. Gozen and O. B. Ozdoganlar, "Design and evaluation of a mechanical nanomanufacturing system for nanomilling," *Precis. Eng.*, vol. 36, no. 1, pp. 19–30, 2012.

[7] A. A. Eielsen, M. Vagia, J. T. Gravdahl, and K. Y. Pettersen, "Damping and tracking control schemes for nanopositioning," *IEEE/ASME Trans. Mechatron.*, vol. 19, no. 2, pp. 432–444, Apr. 2014.

[8] A. J. Fleming and K. K. Leang, "Charge drives for scanning probe microscope positioning stages," *Ultramicroscopy*, vol. 108, no. 12, pp. 1551–1557, 2008.

[9] A. J. Fleming, S. Aphale, and S. O. R. Moheimani, "A new method for robust damping and tracking control of scanning probe microscope positioning stages," *IEEE Trans. Nanotechnol.*, vol. 9, no. 4, pp. 438–448, Jul. 2010.

[10] G. Y. Gu and L. M. Zhu, "Comparative experiments regarding approaches to feedforward hysteresis compensation for piezoceramic actuators," *Smart Mater. Struct.*, vol. 23, no. 9, pp. 095029-1–095029-11, 2014.

[11] S. Xiao and Y. Li, "Modeling and high dynamic compensating the rate-dependent hysteresis of piezoelectric actuators via a novel modified inverse Preisach model," *IEEE Trans. Control Syst. Technol.*, vol. 21, no. 5, pp. 1549–1557, Sep. 2013.

[12] P. Krejci and K. Kuhnen, "Inverse control of systems with hysteresis and creep," *IEE Proc. Control Theory Appl.*, vol. 148, no. 3, pp. 185–192, 2001.

[13] G. Y. Gu, L. M. Zhu, and C. Y. Su, "Modeling and compensation of asymmetric hysteresis nonlinearity for piezoceramic actuators with a modified Prandtl-Ishlinskii model," *IEEE Trans. Ind. Electron.*, vol. 61, no. 3, pp. 1583–1595, Mar. 2014.

[14] C. J. Lin and P. T. Lin, "Tracking control of a biaxial piezo-actuated positioning stage using generalized duhem model," *Comput. Math. Appl.*, vol. 64, no. 5, pp. 766–787, 2012.

[15] M. Rakotondrabe, "Bouc–Wen modeling and inverse multiplicative structure to compensate hysteresis nonlinearity in piezoelectric actuators," *IEEE Trans. Autom. Sci. Eng.*, vol. 8, no. 2, pp. 428–431, Apr. 2011.

[16] S. Devasia, E. Eleftheriou, and S. O. R. Moheimani, "A survey of control issues in nanopositioning," *IEEE Trans. Control Syst. Technol.*, vol. 15, no. 5, pp. 802–823, Sep. 2007.

[17] G. Song, J. Q. Zhao, X. Q. Zhou, and J. A. D. Abreu-Garcia, "Tracking control of a piezoceramic actuator with hysteresis compensation using inverse Preisach model," *IEEE/ASME Trans. Mechatron.*, vol. 10, no. 2, pp. 198–209, Apr. 2005.

[18] Y. Shan and K. K. Leang, "Accounting for hysteresis in repetitive control design: Nanopositioning example," *Automatica*, vol. 48, no. 4, pp. 1751–1758, 2012.
[19] A. Esbrook, X. Tan, and H. K. Khalil, "Control of systems with hysteresis via servocompensation and its application to nanopositioning," *IEEE Trans. Control Syst. Technol.*, vol. 21, no. 3, pp. 725–738, May 2013.
[20] H. Habibullah, H. R. Pota, I. R. Petersen, and M. S. Rana, "Tracking of triangular reference signals using lqg controllers for lateral positioning of an AFM scanner stage," *IEEE/ASME Trans. Mechatron.*, vol. 19, no. 4, pp. 1105–1114, Aug. 2014.
[21] A. Sebastian and S. Salapaka, "Design methodologies for robust nanopositioning," *IEEE Trans. Control Syst. Technol.*, vol. 13, no. 6, pp. 868–876, Nov. 2005.
[22] G. Y. Gu, L. M. Zhu, and C. Y. Su, "High-precision control of piezoelectric nanopositioning stages using hysteresis compensator and disturbance observer," *Smart Mater. Struct.*, vol. 23, no. 10, pp. 105007-1–105007-10, 2014.
[23] H. C. Liaw, B. Shirinzadeh, and J. Smith, "Enhanced sliding mode motion tracking control of piezoelectric actuators," *Sens. Actuators A, Phys.*, vol. 138, no. 1, pp. 194–202, 2007.
[24] J. C. Shen, W. Y. Jywe, and C. H. Liu, "Sliding-mode control of a three-degrees-of-freedom nanopositioner," *Asian J. Control*, vol. 10, no. 3, pp. 267–276, 2008.
[25] Q. Xu and Y. Li, "Micro-/nanopositioning using model predictive output integral discrete sliding mode control," *IEEE Trans. Ind. Electron.*, vol. 59, no. 2, pp. 1161–1170, Feb. 2012.
[26] J. Y. Peng and X. B. Chen, "Integrated PID-based sliding mode state estimation and control for piezoelectric actuators," *IEEE/ASME Trans. Mechatron.*, vol. 19, no. 1, pp. 88–99, Feb. 2014.
[27] G. Y. Gu, L. M. Zhu, C. Y. Su, and H. Ding, "Motion control of piezoelectric positioning stages: Modeling, controller design and experimental evaluation," *IEEE/ASME Trans. Mechatronics*, vol. 18, no. 5, pp. 1459–1471, Oct. 2013.
[28] Q. Xu and Y. Li, "Model predictive discrete-time sliding mode control of a nanopositioning piezostage without modeling hysteresis," *IEEE Trans. Control Syst. Technol.*, vol. 20, no. 4, pp. 983–994, Jul. 2012.
[29] R. Kikuuwe and H. Fujimoto, "Proxy-based sliding mode control for accurate and safe position control," in *Proc. IEEE Int. Conf. Robot. Autom.*, 2006, pp. 25–30.
[30] M. Edardar, X. Tan, and H. K. Khalil, "Sliding-mode tracking control of piezo-actuated nanopositioners," in *Proc. Amer. Control Conf.*, 2012, pp. 3825–3830.
[31] G. Y. Gu and L. M. Zhu, "Motion control of piezoceramic actuators with creep, hysteresis and vibration compensation," *Sens. Actuators A, Phys.*, vol. 197, pp. 76–87, 2013.
[32] R. Kikuuwe, S. Yasukouchi, H. Fujimoto, and M. Yamamoto, "Proxy-based sliding mode control: a safer extension of pid position control," *IEEE Trans. Robot.*, vol. 26, no. 4, pp. 670–683, Aug. 2010.
[33] J.-J. E. Slotine and W. Li, *Applied Nonlinear Control*. Englewood Cliffs, NJ, USA: Prentice-Hall, 1991.
[34] M. Van Damme, B. Vanderborght, B. Verrelst, R. Van Ham, F. Daerden, and D. Lefeber, "Proxy-based sliding mode control of a planar pneumatic manipulator," *Int. J. Robot. Res.*, vol. 28, no. 2, pp. 266–284, 2009.
[35] R. Kikuuwe, "A sliding-mode-like position controller for admittance control with bounded actuator force," *IEEE/ASME Trans. Mechatron.*, vol. 19, no. 5, pp. 1489–1500, Oct. 2014.
[36] K. H. Ang, G. Chong, and Y. Li, "PID control system analysis, design, and technology," *IEEE Trans. Control Syst. Technol.*, vol. 13, no. 4, pp. 559–576, Jul. 2005.
[37] C. X. Li, G. Y. Gu, M. J. Yang, and L. M. Zhu, "Design, analysis and testing of a parallel-kinematic high-bandwidth xy nanopositioning stage," *Rev. Sci. Instrum.*, vol. 84, no. 12, pp. 125111-1–125111-12, 2013.
[38] B. Kristiansson and B. Lennartson, "Robust tuning of PI and PID controllers," *IEEE Control Syst. Mag.*, vol. 26, no. 1, pp. 55–69, Feb. 2006.
[39] C. Jin, K. Ryu, S. Sung, J. Lee, and I. Lee, "PID auto-tuning using new model reduction method and explicit PID tuning rule for a fractional order plus time delay model," *J. Proc. Cont.*, vol. 24, no. 1, pp. 113–118, 2014.
[40] W. K. Ho, K. W. Lim, and W. Xu, "Optimal gain and phase margin tuning for PID controllers," *Automatica*, vol. 34, no. 8, pp. 1009–1014, 1998.

**Guo-Ying Gu** (S'10–M'13) received the B.E. degree (with hons.) in electronic science and technology, and the Ph.D. degree (with hons.) in mechatronic engineering from Shanghai Jiao Tong University (SJTU), Shanghai, China, in 2006 and 2012, respectively.

From October 2010 to March 2011 and from November 2011 to March 2012, he was a Visiting Researcher at Concordia University, Montreal, QC, Canada. Since October 2012, he has been working at SJTU, where he is currently appointed as a Lecturer with the Faculty of School of Mechanical Engineering. Supported by the Alexander von Humboldt Foundation, he was at the University of Oldenburg, Oldenburg, Germany, from August 2013 to July 2014, on leave from SJTU. His research interests include robotics and equipment automation, design and high-bandwidth control of nanopositioning stages, and modeling and control of systems involving with hysteresis. He has published more than 30 peer-reviewed papers, including 20 SCI-indexed journal papers.

Dr. Gu received the Best Conference Paper Award of the 2011 IEEE International Conference on Information and Automation in 2011, Scholarship Award for Excellent Doctoral Student granted by Ministry of Education of China in 2011, Hiwin Excellent Mechanical Doctoral Dissertation Award of China in 2013, and Alexander von Humboldt Fellowship in 2013. He has severed as the Guest Editor of the special issue on Micro/Nano Mechatronics and Automation in *International Journal of Advanced Robotic Systems*. He has also severed for several conferences as an international program Committee Member.

**Li-Min Zhu** (M'12) received the B.E. degree (with hons.) and the Ph.D. degree in mechanical engineering from Southeast University, Nanjing, China, in 1994 and 1999, respectively.

From November 1999 to January 2002, he was a Postdoctoral Fellow in the Huazhong University of Science and Technology. Since March 2002, he has been with Shanghai Jiao Tong University, Shanghai, China, where he is currently a Distinguished Professor and the Vice Director of the State Key Laboratory of Mechanical System and Vibration. His research interests include 1) fixturing, CNC machining and 3-D measurement of complex shaped parts and 2) control, sensing and instrumentation for micro/nano manufacturing. He has published one monograph and more than 170 peer-reviewed papers, including 95 on international journals.

Dr. Zhu received the National Distinguished Youth Scientific Fund of China in 2013. Now he serves as the Associate Editor of the IEEE TRANSACTIONS ON AUTOMATION SCIENCE AND ENGINEERING, and the Editorial Board Member of Proceedings of the IMechE, Part B: Journal of Engineering Manufacture.

**Chun-Yi Su** (SM'98) received the Ph.D. degree in control engineering from the South China University of Technology, Guangzhou, China, in 1990.

After a seven-year stint at the University of Victoria, he joined the Concordia University, Montreal, QC, Canada, in 1998, where he is currently a Professor of mechanical and industrial engineering and holds the Concordia Research Chair in Control. He has also held several short-time visiting positions including a Chang Jiang Chair Professorship by Chinas Ministry of Education and JSPS Invitation Fellowship from Japan. His research interests include control theory and its applications to various mechanical systems, with a recent focus on control of systems involving hysteresis nonlinearities. He is the author or coauthor of more than 300 publications, which have appeared in journals, as book chapters and in conference proceedings.

Dr. Su has served as an Associate Editor of IEEE TRANSACTIONS ON AUTOMATIC CONTROL and IEEE TRANSACTIONS ON CONTROL SYSTEMS TECHNOLOGY. He has been on the Editorial Board of 18 journals, including *IFACs Control Engineering Practice and Mechatronics*. He has also severed for many conferences as an Organizing Committee Member, including General Cochair of the 2012 IEEE International Conference on Mechatronics and Automation and Program Chair of the 2007 IEEE Conference on Control Applications.

**Han Ding** (M'97–SM'00) received the Ph.D. degree from the Huazhong University of Science and Technology (HUST) , Wuhan, China, in 1989.

Supported by the Alexander von Humboldt Foundation, he was with the University of Stuttgart, Stuttgart, Germany, from 1993 to 1994. He was with the School of Electrical and Electronic Engineering, Nanyang Technological University, Singapore from 1994 to 1996. He has been a Professor at HUST since 1997. He is the Director of State Key Lab of Digital Manufacturing Equipment and Technology at HUST and a "Cheung Kong" Chair Professor of Shanghai Jiao Tong University. He was elected as a Member of the Chinese Academy of Sciences in 2013. His research interests include robotics, multiaxis machining, and equipment automation.

Dr. Ding is currently the Editor of IEEE TRANSACTIONS ON AUTOMATION SCIENCE AND ENGINEERING, and the Technical Editor of IEEE/ASME TRANSACTIONS ON MECHATRONICS. He serves as a Guest Editor and a Technical Committee Member of semiconductor manufacturing automation in IEEE RA society. He has also organized and chaired many technical sessions and workshops in various international conferences.

**Sergej Fatikow** (M'98) studied electrical engineering and computer science at the Ufa Aviation Technical University, Ufa, Russia, where he received the doctoral degree in 1988 with work on fuzzy control of complex nonlinear systems.

From 1988 to 1990, he was a Lecturer at Ufa Aviation Technical University, where he became an Assistant Professor in 1996. In 2000, he became an Associate Professor at the University of Kassel, Germany. Since 2001, he has been a Full Professor in the Department of Computing Science, University of Oldenburg, Oldenburg, Germany, where he is also the Head of Technology Cluster Automated Nanohandling at the Research Institute for Information Technology. Since 1990, he published more than 120 book chapters and journal papers and more than 250 conference papers. His research interests include micro- and nano-robotics, automated robot-based nanohandling in scanning electron microscope, micro- and nano-assembly, atomic force microscopy-based nanohandling, sensor feedback on the nanoscale, and neurofuzzy robot control.

Dr. Fatikow is the Founding Chair of the International Conference on Manipulation, Manufacturing and Measurement on the Nanoscale (3M-NANO), the Europe-Chair of IEEE-RAS Technical Committee on Micro/Nano Robotics and Automation, and the Executive President of 3M-NANO International Society.